

KINEMATIC MODEL FOR ECLIPSE AND ECLIPSE-II PARALLEL ROBOT.

Henrique Simas, hsimas@univali.br

UNIVALI – CE São José, Rod. SC 407, km 04 , Sertão do Imaruim São José, SC, CEP 88022-000

Altamir Dias, altamir@emc.ufsc.br

Daniel Martins, daniel@emc.ufsc.br

EMC - Universidade Federal de Santa Catarina – Campus Trindade, Florianópolis – SC, CEP 88040-970

Abstract. *In general, the first choice for inverse kinematics solution of robots is analytical methodologies, based on geometric intuition. But the geometric intuition sometimes fails when the kinematic structures become increasingly complex, this is most evident robots with parallel structure. Some references presents analytical solutions for the position and differential kinematics for parallel robots, but generally the kinematics concepts of these robots are simple to understand. Parallel robots as the Eclipse and Eclipse-II are considered as complex kinematics chain and the solution of the position and velocity kinematics are obtained by analytical methods, using for both geometric analysis for some particular situation. This paper proposes a model to differential kinematics for robots Eclipse and Eclipse-II, using the method of Assur virtual chains. The use of virtual chains allows to formal systematic solution for kinematics and the use of a integration method based on the control of the closure error measured. It discussed the Screw theory, Assur virtual chain, differential model, the numerical integration method, and in the final, is presented a study of singularities and a simulation of a planned trajectory to validate the proposed model*

Keywords: *Parallel robots, complex kinematic chains, Assur virtual chain, singularity analysis.*

1. INTRODUCTION

Parallel mechanism is actually an area of interest for industrial applications and advanced researches. The advances in informatics technology and the development of more accurate methods, allows a rapid increasingly of parallel robots daily of production systems.

This paper discusses a solution for the position and velocity kinematics of parallel robots Eclipse and Eclipse-II.

The Eclipse parallel robot was presented by Kim and Park (1998), as a result of a design study for a kinematics which allow operations in 360° in its workspace. The robot Eclipse-II was first presented 2002 (Kim, 2002), showing itself as an evolution of the Eclipse and with the objective to be used in flight simulators. The advantage of this kinematic structure for the design of flight simulators, is the possibility of movements in 360° in its workspace. The forward and inverse kinematics discussed on these papers are based on geometric approaches, as well as the singularities analysis. References present alternative solution using still based on geometric treatment (Liu, 2003) (Altuzarra 2004). Other references treat just the forward kinematics as in Wang (2006). The proposals methods for obtaining the differential kinematics are don't have a systematic way, in general are resolved in a particular way for each case.

In parallel robots, singular condition occurs in forward and inverse kinematics (Gosselin, 1990). Its identification can be obtained through kinematic differential models, and this analysis requires a consistent differential kinematic model. Singularities are discussed from the geometric analysis (Gregorio, 2002), and Antazurra (2004) presents a study which is a classification of singularities in closed kinematic chains.

This work proposes a systematic model to differential kinematics for robots Eclipse and Eclipse-II, using the method of Assur virtual chains (Campos, 2005). The use of virtual chains allows applying a method of integration based on the control of the closure error measured (Simas, 2008). It discusses the differential model, the numerical integration method, and in the final, is presented a study of singularities and a simulation of a planned trajectory to validate the proposed model. The major proposes of this paper is contribute with the study of kinematic problem of parallel robots, applying the results to a complex kinematic robots, Eclipse and Eclipse-II, and discuss a way to alternative analysis of singularity condition.

2. THEORETICAL REVIEW

The description of the differential kinematics of robots Eclipse and Eclipse II are based on screw representation and in a use of Assur virtual chains. Additionally we used the Davies' method to describe the inverse kinematics of closed chains, and analysis of graphs to investigate the relationship of movement in a joint. These concepts are described shortly in following.

2.1. Screw representation of differential kinematics

The general spatial differential movement of a rigid body consists of a differential rotation about, and a differential translation along an axis named the instantaneous screw axis. In this way the velocities of the points of a rigid body with respect to an inertial reference frame $O-xyz$ may be represented by a differential rotation ω about the instantaneous screw axis and a simultaneously differential translation τ about this axis. The complete movement of the rigid body, combining rotation and translation, is called screw movement or twist and is here denoted by $\$$. Fig. 1 shows a body “twisting” around the instantaneous screw axis. The ratio of the linear velocity to the angular velocity is called the pitch of the screw $h = |\tau|/|\omega|$.

The twist may be expressed by a pair of vectors, i.e. $\$ = [\omega^T; V_p^T]^T$, where ω represents the angular velocity of the body with respect to the inertial frame, and V_p represents the linear velocity of a point P attached to the body which is instantaneously coincident with the origin O of the reference frame. A twist may be decomposed into its magnitude and its corresponding normalized screw. The twist magnitude, denoted as \dot{q} in this study, is either the magnitude of the angular velocity of the body, $|\omega|$, if the kinematic pair is rotative or helical, or the magnitude of the linear velocity, $|V_p|$, if the kinematic pair is prismatic. The normalized screw, $\hat{\$}$, is a twist in which the magnitude is factored out, i.e.

$$\$ = \hat{\$} \dot{q} \tag{1}$$

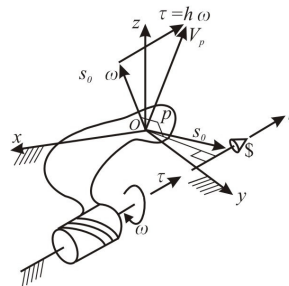


Figure 1. Screw movement or twist.

The normalized screw coordinates (Davidson, 2004) may be given by,

$$\hat{\$} = \begin{bmatrix} s \\ s_0 \times s + hs \end{bmatrix} \tag{2}$$

where, as above, the vector $s = [s_x \ s_y \ s_z]^T$ denotes a unit vector along the direction of the screw axis, and the vector $s_0 = [s_{0x} \ s_{0y} \ s_{0z}]^T$ denotes the position vector of a point lying on the screw axis.

Thus, the twist given in Eq. (1) expresses the general spatial differential movement (velocity) of a rigid body with respect to an inertial reference frame $O-xyz$. The twist can also represent the movement between two adjacent links of a kinematic chain. In this case, the twist $\$_i$ represents the movement of link i with respect to link $(i-1)$.

2.2. Davies’ method

Davies’ method is a systematic way to relate the joint velocities in closed kinematic chains. Davies (Campos 2001) derives a solution to the differential kinematics of closed kinematic chains from the Kirchhoff circulation law for electrical circuits. The resulting Kirchhoff-Davies circulation law states that “The algebraic sum of relative velocities of kinematic pairs along any closed kinematic chain is zero”⁵.

We use this law to obtain the relationship between the velocities of a closed kinematic chain¹. Thus, considering that the velocity of a link with respect to itself is null, the circulation law can be expressed as

$$\sum_{i=1}^n \$_i = 0 \tag{3}$$

where 0 is a vector the dimension of which corresponds to the dimension of the twist $\$_i$.

According to the normalized screw definition introduced above, Eq.(2) may be rewritten as

$$\sum_{i=1}^n \hat{\$}_i \dot{q}_i = 0 \tag{4}$$

where \hat{S}_i and \dot{q}_i represent the normalized screw and the magnitude of twist S_i , respectively.

Equation (4) is the constraint equation which, in general can be written as

$$N\dot{q} = 0 \tag{5}$$

where $N=[\hat{S}_1 \ \hat{S}_2 \ \dots \ \hat{S}_n]$ is the network matrix containing the normalized screws, the signs of which are dependent on the screw definition in the circuit orientation, and $\dot{q} = [\dot{q}_1 \ \dot{q}_2 \ \dots \ \dot{q}_n]$ is the magnitude vector.

A closed kinematic chain has actuated joints, here named primary joints, and passive joints, named secondary joints. The constraint equation, Eq. (5), allows the calculation of the secondary joint velocities as functions of the primary joint velocities. To this end, the constraint equation is rearranged highlighting the primary and secondary joint velocities and Eq. (5) is rewritten as follows:

$$\begin{bmatrix} N_p & \vdots & N_s \\ \dot{q}_p & \dots & \dot{q}_s \end{bmatrix} = 0 \tag{6}$$

where N_p and N_s are the primary and secondary network matrices, respectively, and \dot{q}_p and \dot{q}_s are the corresponding primary and secondary magnitude vectors, respectively.

Equation (6) can be rewritten as

$$N_p\dot{q}_p + N_s\dot{q}_s = 0 \tag{7}$$

The secondary joint position can be calculated by integrating Eq. (7) as follows:

$$q_s(t) - q_s(0) = \int_0^t \dot{q}_s dt = - \int_0^t N_s^{-1} N_p \dot{q}_p dt \tag{8}$$

2.3. Assur virtual chain

The Assur virtual kinematic chain concept, virtual chain for short, is essentially a tool to obtain information on the movement of a kinematic chain or to impose movements on a kinematic chain (Campos, 2005).

This concept was first introduced by Campos *et al* (2005), which defines the virtual chain as a kinematic chain composed of links (virtual links) and joints (virtual joints) and which possesses the following three properties: a) the virtual chain is open; b) it has joints whose normalized screws are linearly independent; and c) it does not change the mobility of the real kinematic chain, in other words, it is an Assur group (Artobolevski, 1977).

From the property c) the virtual chain proposed by Campos *et al.*(2005) is in fact an Assur group, i.e. a kinematic subchain with null mobility that when connected to another kinematic chain preserves mobility. To represent the movements in the Cartesian system the 3P3R chain is used.

The 3P3R virtual chain is composed of three orthogonal prismatic joints (in the x, y, and z directions), and a spherical wrist, composed of three rotative joints (in the x, y, and z directions). Fig. 2 shows the 3P3R Assur virtual chain with the virtual links C_i labeled.

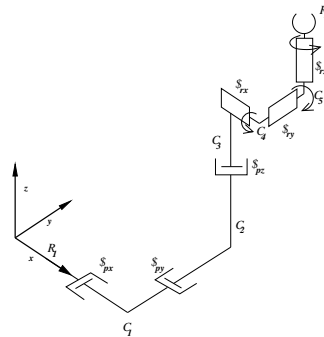


Figure 2. 3P3R Assur virtual chain.

Other Assur virtual chains can be founded in Artobolevski (1977) and Davidson (2004).

2.4. The direct graph notation

Consider a kinematic pair composed of two links E_i and E_{i+1} . This kinematic pair has the relative velocity defined for a screw ${}^R\mathcal{S}_j$ (joint j) in relation to a reference frame R . The joint j represents the relative movement of the link E_i with respect to the link E_{i+1} . This relation can be represented as a graph, as shown Fig. 3(a).

Where vertices represent links and arcs represent joints. The relative movement is also indicated by the arcs directions. For instance in Fig. 3(a), the link E_{i+1} moves with respect to link E_i via the joint j .

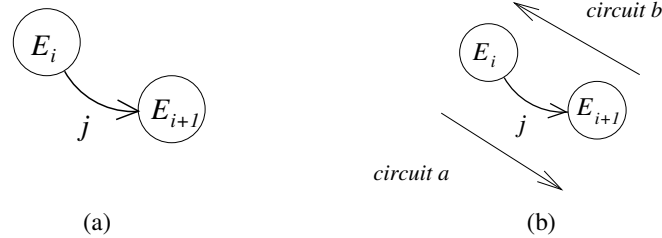


Figure 3. (a) relative movement of link E_i with respect to link E_{i+1} represented graphically;
 (b) relation between joint j and the *circuits a* and *b*.

Now consider the following example, where the joint j is part of two closed chains. For each closed chain the circuit direction is defined (Campos, 2005). Fig. 3(b) shows an example.

In a direct mechanism graph, if the joint has the same direction as the circuit, the twist associated with the joint has a positive sign in the circuit equation (Eq. (13)), and, if the joint has the opposite direction to the circuit, the sign will be negative.

In the example the twist ${}^R\mathcal{S}_j$, associated with the joint j , will have a positive sign in the *circuit a* equation and a negative sign in the *circuit b* equation.

2.5. Integration algorithm using Assur virtual chains

Simas (2008) presents a new integration algorithm integrate the differential kinematics equation to obtain the joint positions. The algorithm proposed has two steps. The first step is to introduce a virtual chain to represent the closure error.

The constraint equation of this closed-loop chain results in:

$$N_p \dot{q}_p + N_s \dot{q}_s + N_e \dot{q}_e = 0 \quad (9)$$

where N_p and N_s are the primary and secondary network matrices obtained by integration, \dot{q}_p and \dot{q}_s are the primary and secondary magnitude vectors, respectively, N_e is the error network matrix, and \dot{q}_e is the error magnitude vector.

The second step is isolate the secondary magnitude vector to replace Eq. (9) by

$$\dot{q}_s = -N_s^{-1} N_p \dot{q}_p + N_s^{-1} N_e K_e q_e \quad (10)$$

where the gain matrix K_e is chosen to be positive definite and q_e is the position error vector.

Applying the Euler integration method in Eq. (10) we obtain:

$$q_s(t_k) = q_s(t_{k-1}) - N_s^{-1}(t_{k-1}) N_p(t_{k-1}) \dot{q}_p \Delta t + N_s^{-1}(t_{k-1}) N_e(t_{k-1}) K_e q_e \Delta t \quad (11)$$

The proposed method is stable and allows the execution of several iterations until an admissible error is within the admissible tolerance (Simas, 2008). To uses this proposed method its necessary obtain the position error vector, that will be treated in the next subsection.

2.6. Position error vector

The screw displacement of a link in a kinematic chain can be expressed by a homogeneous matrix, and the resultant screw displacement in a link j can be calculated using the successive screw displacement method by premultiplying the homogeneous matrices corresponding to the preceding joint motions, i.e.

$$A_j = \prod_{i=1}^{j-1} A_i \quad (12)$$

As in a closed loop chain, the first and the last links are the same, and the orientation and position of a link with respect to itself are given by a homogeneous matrix equal to the fourth-order identity matrix. In a closed-loop chain with np primary joints and ns secondary joints Eq.(12) the closed-loop equation results in:

$$\prod_{i=1}^{np} [A_p]_i \prod_{i=1}^{ns} [A_s]_i = I \quad (13)$$

where $[A_p]_i, i = 1 \dots np$ are the homogeneous matrices corresponding to the primary joints, and $[A_s]_i, i = 1 \dots ns$ are the homogeneous matrices corresponding to the secondary joints.

We represent the closure error with a homogeneous matrix E , and the closed-loop equation becomes

$$\left\{ \prod_{i=1}^{np} [A_p]_i \prod_{i=1}^{ns} [A_s]_i \right\} E = I \quad (14)$$

The closure error is calculated by

$$E = \left\{ \prod_{i=1}^{np} [A_p]_i \prod_{i=1}^{ns} [A_s]_i \right\}^{-1} = \begin{bmatrix} R_e & p_e \\ 0 & 1 \end{bmatrix} \quad (15)$$

where $p_e = [p_{ex} \ p_{ey} \ p_{ez}]^T$ is the position error vector and R_e is the rotation matrix error. The matrix R_e corresponds to errors measured in r_{ex}, r_{ey} and r_{ez} virtual rotative joints considering their structural conception.

The “position” error (which is a posture error involving position and orientation) is given by the position error vector $q_e = [r_{ex} \ r_{ey} \ r_{ez} \ p_{ex} \ p_{ey} \ p_{ez}]^T$.

3. DIFFERENTIAL KINEMATICS MODELS

3.1. Eclipse and Eclipse-II kinematic structures

Eclipse (Fig. 4) design consists of three *PPRS* serial subchains (*P*, *R*, and *S* here denote prismatic, revolute, and spherical joints respectively), with the first *P* joint denoting sliding motion along the circular guideway. The mechanism has six kinematic degrees of freedom; with the actuated joints are the prismatic joints (Park, 2001). The three kinematic subchains are connected to a triangular moving plate through *S* joints.

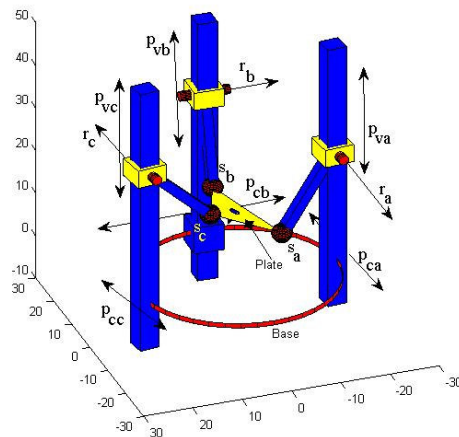


Figure 4. Eclipse kinematic conception.

In Fig. 4, each subchain is indicated by the letters *a*, *b* and *c*; p_{vj}, p_{vj}, r_j and s_j are the circular prismatic joint, vertical prismatic joint, rotative joint and spherical joint of subchain $j=a, b, c$ respectively.

The Eclipse-II consists of three *PPRS* serial subchains that move independently on a fixed circular guide. The Eclipse-II has six degrees of freedom and six actuated joints. These joints are the three prismatic joints along the horizontal circular guide, two prismatic joint on the vertical columns, and another prismatic joint on the vertical circular column. All six actuated joints can be found in Fig. 5, and are indicated by arrows. The connecting links are attached to the circular and vertical columns, respectively, through revolute joints. The other ends of these links are mounted to the moving platform via three spherical joints. Mounting one circular column and two linear columns on the circular guide results in the Eclipse II having a large orientation workspace. The Fig. 5 presents the Eclipse-II.

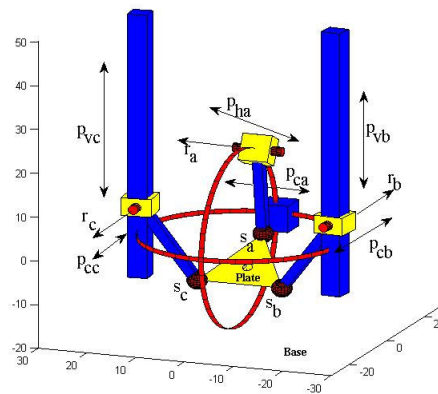


Figure 5. Eclipse-II kinematics structure.

In Fig. 6, the subchains *b* and *c* have the same structure compares with subchains *b* and *c* from Eclipse. The difference is in subchain *a* which the second prismatic joint is mounted in a circular guide, similar to their first joint prismatic. This second joint will be indicated by p_{ha} identifier.

3.2. Modelling the differential kinematics

It was detected that the graph and Davies equation to the models of robots have the same structure. The difference is only in the definition of the screw of the prismatic joint of the second circular guide on the Eclipse-II. So, in following is presented the graph and the Davies that serves to both Eclipse and Eclipse-II.

To define the differential and positions equation, were added an Assur virtual chain to conduct the moving plate, and for each subchain an error virtual chain, each one with six degrees of freedom. The Fig. 6 shows the graph.

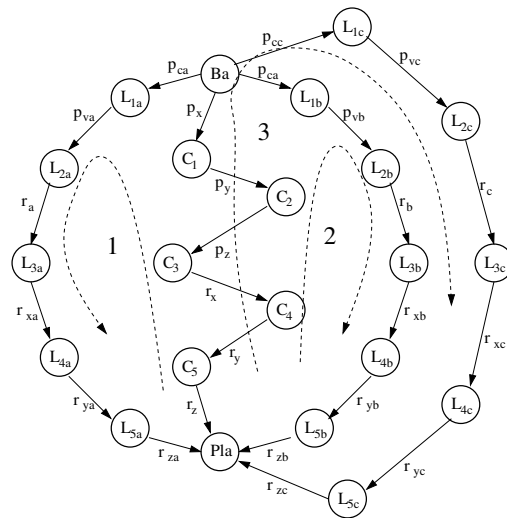


Figure 6. Eclipse and Eclipse-II graph

where L_{ij} indicates the link i on subchain j ; p_{cj} is the prismatic circular joint of the subchain j ; p_{vj} is the prismatic vertical joint of the subchain j ; r_j is the revolute joint of the subchain j and r_{xj}, r_{yj}, r_{zj} are the rotative joint that represent the expansion of the movements from spherical joint of the subchain j .

In agree with the graph and joint disposition, the N_p and N_s matrixes could be obtained. To Eclipse the results are present in Eq. (16)

$$N_s \dot{q}_s + N_p \dot{q}_p = \begin{bmatrix} M_a & 0 & 0 \\ 0 & M_b & 0 \\ 0 & 0 & M_c \end{bmatrix} \begin{bmatrix} \psi_a \\ \psi_b \\ \psi_c \end{bmatrix} + \begin{bmatrix} M_{1a} & 0 & 0 \\ 0 & M_{1b} & 0 \\ 0 & 0 & M_{1c} \end{bmatrix} \begin{bmatrix} \psi_{1a} \\ \psi_{1b} \\ \psi_{1c} \end{bmatrix} = 0 \quad (16)$$

where $M_j = [\hat{s}_{cj} \ \hat{s}_{vj} \ \hat{s}_{rj} \ \hat{s}_{xj} \ \hat{s}_{yj} \ \hat{s}_{zj}]$, is the set of unitary screws of the Eclipse subchain j , respectively to joints p_{cj} , p_{vj} , r_j , r_{xj} , r_{yj} and r_{zj} ; $M_{1j} = [\hat{s}_{px} \ \hat{s}_{py} \ \hat{s}_{pz} \ \hat{s}_{rx} \ \hat{s}_{ry} \ \hat{s}_{rz}]$ is the set of unitary screws of the virtual chain responsible by the trajectory generation of each Eclipse subchain; and the vectors ψ_j and ψ_{1j} are the velocities magnitudes from each i Eclipse subchain and from each j trajectory virtual chain, respectively.

Must be explained that the five firstly screws from trajectory Assur virtual chains, are the same for the Eclipse subchains a , b and c . The sixthly screw, that represents the relative movement of the z-axis from 3P3R trajectory Assur virtual chain, is different to each Eclipse subchain. Depends on the shape of the end-effector plate, the z-axis must be summed of an angle, or a phase. The model here developed considers the end-effector plate an equilateral triangle and so the z-axis for each Eclipse subchain has summed phases 0° , 120° and -120° respectively for subchain a , b and c . For this reason the model just the screw \hat{s}_{rj} has indicated the indices j .

To Eclipse-II has the graph structure presented on Fig. 6, with the difference on second joint of the subchain a . is substituted for the p_{ha} joint (for more details see Fig. 5). Consequently the circuit equation has the structure as shown in Eq(16), with the difference in M_a submatrix where the screw \hat{s}_{va} is substituted for the \hat{s}_{ha} .

4. SINGULARITY ANALYSIS

The complexity of the kinematic chain of the Eclipse and Eclipse-II are discussed by Kim, (1998) and Kim (2001) respectively. The singularities discusses about singularities are based on a geometric analysis and numerical approaches. The model presented on previous section allows to determinate the singularity condition for the forward and inverse kinematics.

4.1 Inverse singularity analysis

Observing the matrix structure presented on Eq (16), it can be seen that the secondary matrix are constituted of a set of submatrix disposed along of the principal diagonal. So, the inverse kinematic singularities can be evaluated calculating the determinant of submatrix M_j , that have the same structure for each subchain. The equation (17) shows this determinant.

$$D(M_j) = r(-r_g + r \cos(q_{rj})) \cos(q_{yj}) \sin(q_{rj}) \quad (17)$$

where q_{rj} is the position angle of the joint r_j ; r is the length of the link connected on vertical prismatic joint p_{vj} and connected to the plate by the spherical s_j joint and r_g is the distance from the base to circular guide.

From the Eq (16) presented can be observed that the singularity conditions occur for the following conditions:

- $q_{rj}=0$ rad;
- $q_{yj}=\pi/2$ rad;
- $r \cos(q_{rj})=r_g$.

This condition is similar to each subchain j for the Eclipse and for the subchain b and c for the Eclipse-II. Further analysis is performed for the subchain a of the Eclipse-II robot.

Calculating the determinant of the submatrix of the Eclipse-II subchain a , has the following result:

$$D(M_a) = r_g r \left(-r_g \cos\left(\frac{L_a}{r_g}\right) + r \cos\left(q_{ra} + \frac{L_a}{r_g}\right) \right) \cos(q_{ya}) \sin(q_{ra}) \quad (18)$$

where L_a is the displacement of the joint p_{ha} .

According to the determinant Eq (17) the subchain a has the following singularities:

- $q_{ra}=0$ rad;
- $q_{ya}=\pi/2$ rad;
- $r \cos\left(q_{ra} + \frac{L_a}{r_g}\right) = r_g \cos\left(\frac{L_a}{r_g}\right)$

4.1 Direct singularity analysis

Once again noting the result shown in Eq(16) can be seen that the primary matrix is constituted of submatrixes arranged on your main diagonal. So, the direct kinematic singularities can be evaluated calculating the determinant of submatrix M_{ii} , that have the same structure for each subchain. The equation (19) shows this determinant.

$$D(M_{ii}) = -\cos(q_{ry}) \tag{19}$$

where q_{dy} is the desired displacement of the rotative r_y joint of the virtual 3P3R trajectory generator chain.

By this way, the singularity occurs when $q_{dy}=\pi/2$. This result is applicable for both Eclipse and Eclipse-II.

The results obtained here can solve both the direct as the inverse kinematics, using for both the numerical algorithm presented in Eq. (15). In the next section numerical simulations are presented to desired trajectory for the robots Eclipse and Eclipse-II.

5. EXPERIMENTAL SIMULATION

To perform the numerical results the following dimension was adopted:

- $r_g=20$ cm
- $r=20$ cm
- Equilateral triangular plate with side = $10\sqrt{3}$ cm

The trajectory was programmed with 100 points, and is constituted of an ellipse in the XY plane together with a variation in Z axis and a constant orientation on X axis and Z axis direction according to the Eq (20).

$$Traj(t) = \begin{cases} x(t) = 5 \cos(2\pi t) \\ y(t) = 3 \sin(2\pi t) \\ z(t) = 10 + \sin(6\pi t) \\ \phi_x = 0.5rad \\ \phi_y = 0rad \\ \phi_z = 0.1rad \end{cases} \quad \text{with } 0 \leq t \leq 1 \text{ and } \Delta t = 0.01 \tag{20}$$

The trajectory is shown in the Fig. 8.

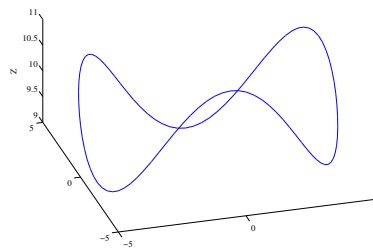


Figure 8. Programmed position trajectory to Eclipse and Eclipse-II

The next figure has shown a sample of a sequence of eight positions to Eclipse.

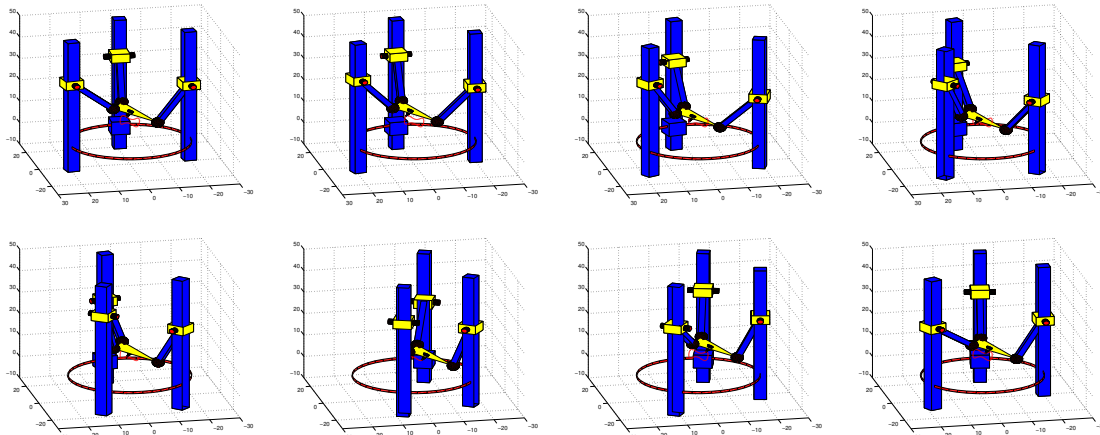


Figure 9. Sequence of eight positions of the robot Eclipse following the planned trajectory

It should be noted that the end-effector movement is performed by the displacement of the vertical prismatic joints and its vertical support columns over the circular guide

Figure 10 presents the profiles of prismatic joints position from the circular guide ring and from the vertical columns.

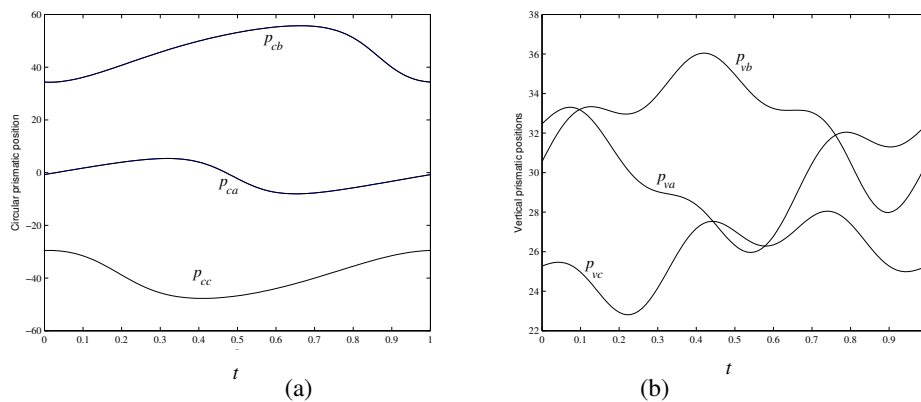


Figure 10. Prismatic joint position: (a) circular guide prismatic joint (b) vertical prismatic joint

Applying the same trajectory for the robot Eclipse-II it has a sample of the sequence of eight positions for the kinematic chain shown in Fig. 11.

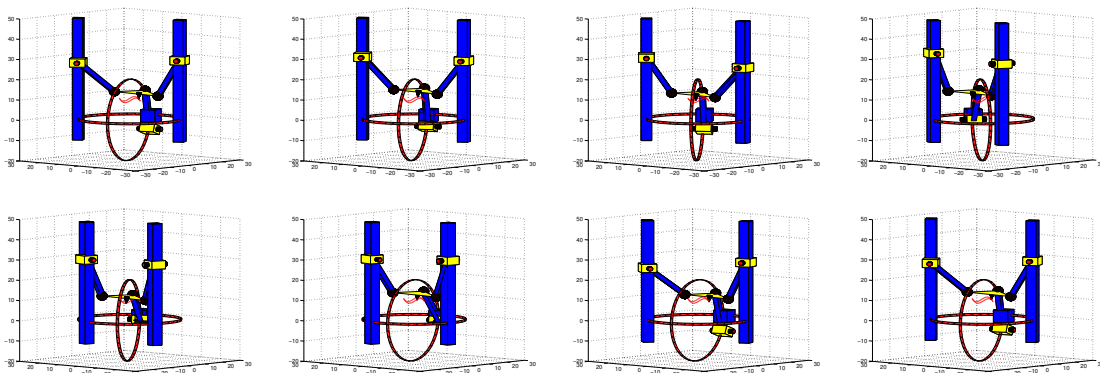


Figure 11. Sequence of eight positions of the robot Eclipse-II following the planned trajectory

Similar to robot Eclipse, the movement of the end-effector is performed by displacement of the three vertical prismatic joints (including a prismatic joint with circular guide), and its respective columns movements in relation with the circular guide in the base. Figure 12 presents the profiles of prismatic joints position from the circular guide ring and from the vertical columns to Eclipse-II.

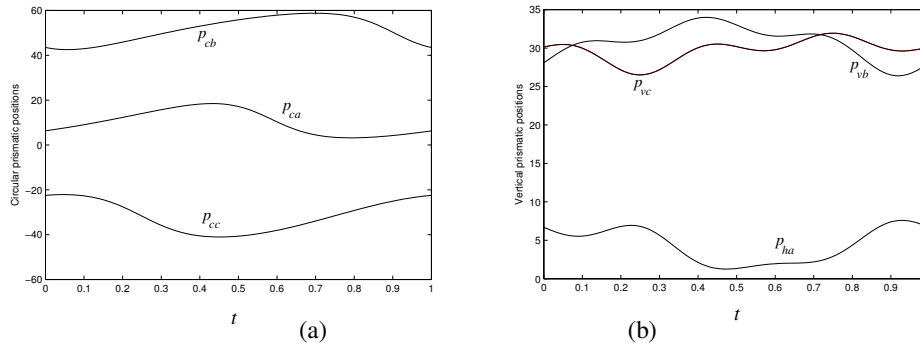


Figure 12. Prismatic joint position to Eclipse-II: (a) circular prismatic joint
 (b) vertical prismatic joint including the circular prismatic joint p_{ha}

3. CONCLUSION

In this paper was presented an alternative kinematic differential model for the parallel robots Eclipse and Eclipse-II. The model discussed was based on Assur virtual chains and its obtaining was shown in a systematic way. Complementary the uses of an integration method, where closure error are controlled, allowed the compute of position joints and so, the references for the robots actuators.

The results allow an implementation of an algorithm to generation of trajectory treating the inverse and forward singularity condition.

The proposed model has the perspective, in the future, to apply on other complex robots, like Adept® Quattro, and PKM® Tricept.

4. REFERENCES

- Altuzarra, O., Pinto, C., Avilés, R. and Hernández, A., 2004, "A Practical procedure to analyze singular configurations in closed kinematic chains", IEEE Trans. on Robotics, Vol 20, No 6.
- Artobolevski, I.I., 1977 "Théorie des Mécanismes et des Machines", Mir Publishers, Moscow.
- Campos, A., Guenther R. and Martins D., 2005, "Differential kinematics of serial manipulators using virtual chains," J. Brazilian Soc. Mechanical Sciences & Engineering, Vol 27, No 4, pp. 345-356 .
- Davidson, J. K. and K.H. Hunt, 2004, "Robots and screw theory: applications of kinematics and statics to robotic", Oxford University Press Inc, New York.
- Gosselin, C. and Angeles, J., 1990, "Singularity Analysis of Closed-Loop Kinematic Chains", IEEE Trans. on Robotics and Automation, Vol 6, No 3, pp-281-290.
- Gregorio, R. , 2005, "Forward problem singularities in parallel manipulators which generate SX-YS-ZS structures", Mechanism and Machine Theory, Vol 40, No. 5, pp. 600-612.
- Kim, J. and Park, F.C., 1998, "Eclipse: A new parallel mechanism prototype", Position Paper in Proc First European American Forum on Parallel Kinematic Machines, Milan, Italy.
- Kim, J., Hwang, J. C., Ki, J. S., Iurascu, C. C., Park, F. C. and Cho, Y. M., 2002, "Eclipse II: A New Parallel Mechanism Enabling Continuous 360-Degree Spinning Plus Three-Axis Translational Motions", IEEE Trans. on Robotics and Automation , Vol. 18, No 3, pp. 367-373.
- Liu, G., Lou, Y. and Li, Z., 2003, "Singularities of Parallel Manipulators: A Geometric Treatment" , IEEE Trans. on Robotics and Automation, Vol 19, Issue 4, pp-579-597.
- Simas, H., 2008, "Planejamento de trajetórias e evitamento de colisão em tarefas de manipuladores redundantes operando em ambientes confinados". PhD thesis, Universidade Federal de Santa Catarina.
- Wang, Y., 2006, "An Incremental Method for Forward Kinematics of Parallel Manipulators", Proc. of the IEEE International Conference on Robotics, Automation and Mechantronics, Bangkok, Thailand, pp. 243-247.

5. RESPONSIBILITY NOTICE

The authors are the only responsible for the printed material included in this paper.